High-m Multiple Tearing Modes in Tokamaks: MHD Turbulence Generation, Interaction with the Internal Kink and Sheared Flows

A. Bierwage 1)*, S. Benkadda 2), M. Wakatani 1)†, S. Hamaguchi 3), Q. Yu 4)

1) Graduate School of Energy Science, Kyoto University, Uji, Kyoto, Japan
2) Equipe Dynamique des Systèmes Complexes, UMR 6633 CNRS-Université de Provence, Marseille, France
3) Center for Atomic and Molecular Technologies, Osaka University, Suita, Osaka, Japan
4) Max-Planck-Institut für Plasmaphysik, Euratom Association, Garching, Germany

e-mail contact of main author: hamaguch@ppl.eng.osaka-u.ac.jp

Abstract. Linear instability and nonlinear dynamics of multiple tearing modes (MTMs) are studied with a reduced magnetohydrodynamic (RMHD) model of a large-aspect-ratio tokamak plasma in the limit of zero pressure. When low-order rational surfaces (such as those for $q = 1$ or 2 with q being the safety factor) are in close proximity, tearing modes on the rational surfaces are strongly coupled and exhibit a broad spectrum of positive growth rates with dominant mode numbers around $m_{\rm peak} \sim 10$. It is shown that collisionless double tearing modes (DTMs) due to electron inertia also have similar linear stability characteristics. Nonlinear dynamics associated with fast growing high-m MTMs can affect the evolution of low-m modes. For example, resistive $q = 1$ triple tearing modes (TTMs) generate MHD turbulence in a disrupted annular ring and the turbulence can impede the growth of an internal kink mode at a finite amplitude. Possible interactions between MTMs and sheared zonal flow are also discussed.

1. Introduction

In discharges with a non-monotonic current profile the profile of the safety factor q maintains an off-axis minimum $q_{\rm min}$ after the current ramp-up. Such configurations have attracted much attention due to their favorable confinement properties, in particular, the formation of an internal transport barrier (ITB) [1]. This enhanced reversed-shear (ERS) tokamak scenario is regarded as a strong candidate for demonstrating self-sustained nuclear fusion conditions in ITER, so it is important to understand instabilities that may occur near $q_{\rm min}$, where the ITB usually forms. In this study, we focus on current-driven instabilities, i.e., kink and tearing modes [2, 3], that are known to cause changes in the magnetic topology by driving magnetic reconnection. This may lead to reduced confinement and disruptive instabilities [4], but may also provide paths to other (possibly dynamic) "equilibrium" states.

In ERS-type configurations, there are pairs of resonant surfaces around $q_{\rm min}$. These are known to be unstable to double tearing modes (DTMs) [2]. In general, multiple resonant surfaces may give rise to multiple tearing modes (MTMs). DTMs were studied extensively in experiment, theory and numerical simulation (e.g., Ref. [5] and references therein). The theoretical and numerical studies that have been presented so far include those on resistive DTMs in a static equilibrium, the effects of shear flow, neoclassical effects, and various reconnection mechanisms other than classical resistivity, such as electron inertia and hyper-viscosity. However, in these studies, the focus was mainly on low-m DTMs. Recently, it has been found that high-m modes can become strongly unstable when the distance between neighboring resonances is small [5, 6].

*Present address: Department of Physics & Astronomy, University of California, Irvine CA, U.S.A.
†Deceased.

This paper presents our recent analyses on linear stability and nonlinear dynamics of current-driven MTMs with high poloidal mode numbers $m \sim \mathcal{O}(10)$ in the core region of a tokamak plasma. The physical model is described in Section 2. In Section 3, the properties of both collisional (resistive) and collisionless DTMs (due to electron inertia) are examined and both are shown to exhibit a broad spectrum of unstable modes with growth rates peaking at $m = m_{\rm peak} \sim 10$. A semi-empirical formula for the dependence of $m_{\rm peak}$ on the system parameters is also proposed. The nonlinear dynamics observed in our simulations include (i) enhanced growth of low-m modes in the early nonlinear regime, (ii) an off-axis internal disruption in the region between the resonances, and (iii) subsequent formation of magnetohydrodynamic (MHD) turbulence in the disrupted region. The reconnection dynamics are dominated by modes with $m \sim m_{\rm peak}$ and the lack of dissipation in the collisionless case allows multiple reconnection cycles to occur. The introduction of sheared zonal flow near $q_{\rm min}$ stabilizes DTMs and gives rise to an ideal instability which again is dominated by high-m modes. In Section 4, we consider an equilibrium with three nearby $q_{\rm s} = 1$ resonances to study the interaction between triple tearing modes (TTMs) and the $m = 1$ internal kink mode. Through nonlinear driving by high-m TTMs, the $m = 1$ mode undergoes enhanced growth, and due to TTM-induced turbulence the $m = 1$ mode can saturate at a finite amplitude. These phenomena may be possible causes of some of experimentally observed phenomena related with sawtooth crashes [6, 7], especially, precursor-less fast sawtooth trigger and partial sawtooth crashes (e.g., Ref. [4]).

2. Physical Model

A tokamak plasma can be described by a reduced magnetohydrodynamic (RMHD) model [8] for the evolution of the magnetic flux ψ and the vorticity u, given by

$$\begin{aligned} \partial_t F &= [F, \phi] - \partial_\zeta \phi - S_{\rm Hp}^{-1} F\,, &(1)\\ \partial_t u &= [u, \phi] + [j, \psi] + \partial_\zeta j + Re_{\rm Hp}^{-1} \nabla_\perp^2 u\,. &(2)\end{aligned}$$

under the assumption of incompressibility and zero pressure. The torus is approximated by a periodic cylinder with coordinates (r, ϑ, ζ). The time is measured in units of the poloidal Alfvén time $\tau_{\rm Hp} = (\mu_0 \rho_{\rm m})^{1/2} a/B_0$ and the radial coordinate is normalized by the minor radius a of the plasma. $\rho_{\rm m}$ is the mass density and B_0 the strong axial magnetic field. $F = \psi + d_{\rm e}^2 j$ is the generalized flux function with $d_{\rm e} = (m_{\rm e}/n_{\rm e} e^2)^{1/2}$ being the electron skin depth. ϕ is the electrostatic potential, $j = -\nabla_\perp^2 \psi$ the current density, $u = \nabla_\perp^2 \phi$ the vorticity. Each field variable f is decomposed into an equilibrium part $\overline{f}$ and a perturbation $\widetilde{f}$ as $f(r, \vartheta, \zeta, t) = \overline{f}(r) + \widetilde{f}(r, \vartheta, \zeta, t)$ and expanded into Fourier modes, $\psi_{m,n}$ and $\phi_{m,n}$ with m and n being the poloidal and toroidal mode numbers. We consider only the nonlinear couplings between modes of a single helicity $h = m/n$, so the problem is reduced to two dimensions.

Magnetic reconnection may occur due to either resistivity or electron inertia. It is referred to as collisional or collisionless reconnection depending on the cause. The magnetic Reynolds number $S_{\rm Hp}$ in Eq. (1) is defined by $S_{\rm Hp} = \tau_\eta/\tau_{\rm Hp}$, with $\tau_\eta = a^2\mu_0/\eta_0$ and $\eta_0 = \eta(r = 0)$ being the resistive diffusion time and the electrical resistivity at $r = 0$. In typical nonlinear simulations, $S_{\rm Hp} \sim 10^6 - 10^8$ is used as it is numerically efficient and physically reasonable in the framework of the model used. The kinematic Reynolds number $Re_{\rm Hp}$ in Eq. (2) is defined by $Re_{\rm Hp} = a^2/\nu\tau_{\rm Hp}$, where ν is the kinematic ion viscosity, and set to satisfy the Prandtl number $Pr = S_{\rm Hp}/Re_{\rm Hp} \lesssim 10^{-1}$, so that the effect of viscosity on the instability of the dominant modes may be neglected. Linear analysis

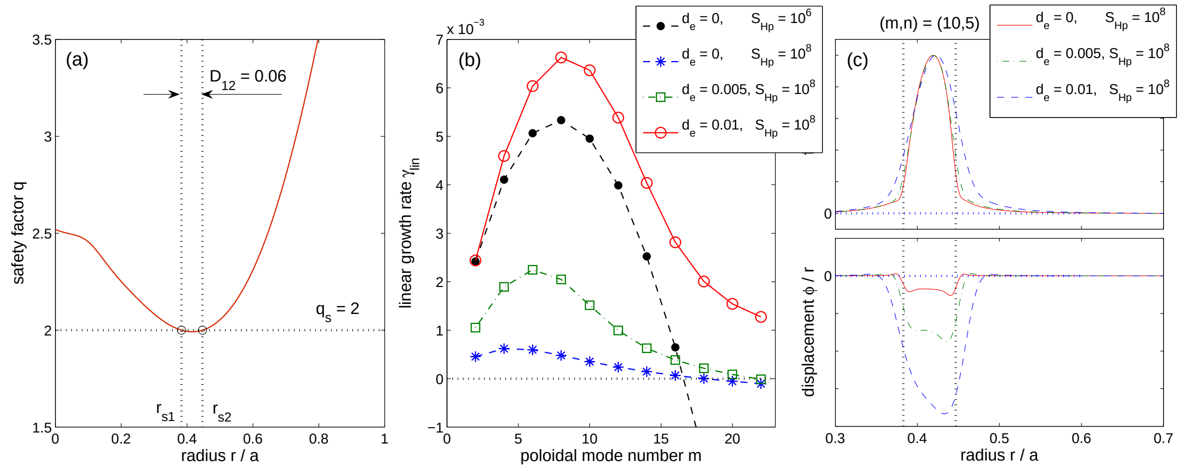

Figure 1: (a): Equilibrium q profile with reversed central shear. (b): Linear growth rate spectra $\gamma_{\rm lin}(m)$ of strongly coupled $q_{\rm s} = 2$ DTMs. Spectra of collisional DTMs ($d_{\rm e} = 0$) are plotted for $S_{\rm Hp} = 10^6$ and $S_{\rm Hp} = 10^8$. Two collisionless cases are shown for $d_{\rm e} = 0.005$ and $d_{\rm e} = 0.01$ ($S_{\rm Hp} = 10^8$). (c): Linear eigenmode structure of a high-m DTM [here, $(m,n) = (10,5)$] for $S_{\rm Hp} = 10^8$ and three values of the electron inertia: $d_{\rm e} = 0$, 0.005, 0.1 (top: flux function ψ; bottom: displacement velocity $v_r \propto \phi/r$).

of Eqs. (1) and (2) is given in Ref. [5]. Nonlinear calculations were carried out with the numerical code described in Ref. [7].

3. Double Tearing Modes (DTMs)

In this Section, DTMs are analyzed for the equilibrium q profile given in Fig. 1(a), where two $q_{\rm s} = 2$ resonant surfaces are separated by a small distance $D_{12} = r_{\rm s2} - r_{\rm s1} = 0.06$. The linear instability and nonlinear evolution of collisional (resistivity-dominated) and collisionless (electron-inertia-dominated) DTMs are presented [9, 10]. In addition, the effect of sheared zonal flow is discussed.

3.1. Spectrum of Unstable Modes and Mode Structures

In Fig. 1(b) the spectra of linear growth rates $\gamma_{\rm lin}(m)$ of strongly coupled DTMs are shown for several values of the magnetic Reynolds number $S_{\rm Hp}$ and electron skin depth $d_{\rm e}$. Both collisional and collisionless DTMs have fast growing modes with $m \sim 10$. The spectrum of collisionless DTMs tends to have a long high-m tail. Resistivity stabilizes modes with very high m; e.g., for $S_{\rm Hp} = 10^6$ modes with $m > m_{\rm max} = 18$ are stable. Electron inertia, in turn, seems to have a destabilizing effect that overcomes the stabilization by small resistivity included in all cases ($S_{\rm Hp} = 10^8$). The mode structure of a typical high-m DTM is shown in Fig. 1(c). Such even-parity eigenmodes are dominant for small D_{12} [5] and there seems to be no significant difference between collisional and collisionless DTMs.

Pritchett, Lee and Drake [11] derived analytical forms for the linear growth rate $\gamma_{\rm lin}$ of DTMs. In the strongly coupled (i.e., $m \cdot D_{12}$ small) and weakly coupled (i.e., $m \cdot D_{12}$ large) limits, the growth rate depends on the poloidal mode number m as

$$\gamma_{\rm lin}^{\rm strong} \propto m^{2/3}, \qquad \gamma_{\rm lin}^{\rm weak} \propto m^{-6/5},$$

Note that the growth rate increases with m in the strong coupling limit whereas it decreases with m in the weak coupling limit. It is also shown in Ref. [11] that, at the

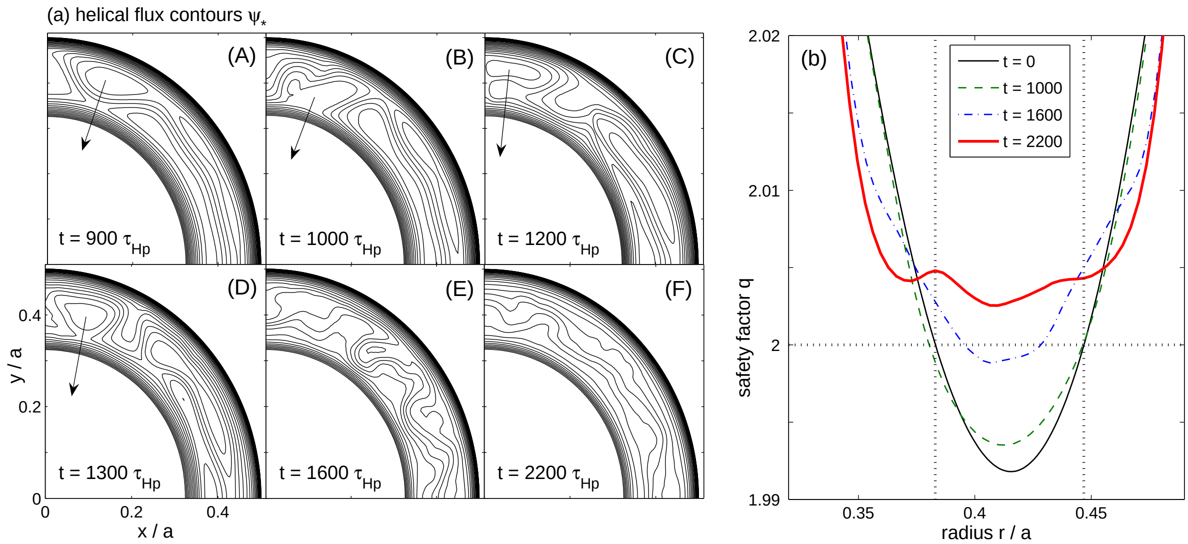

Figure 2: (a) Contour plots of the helical flux $\psi_* = \psi + r^2/(2q_s)$ with $q_s = 2$, showing magnetic reconnection due to collisionless DTMs in the nonlinear regime. The arrows in snapshots (A) and (B) indicate the first reconnection cycle: a primary reconnection event (island formation) and a secondary reconnection event where the same island disappears on the other side of the inter-resonance region. The arrows in snapshot (C) and (D) indicate a second cycle. (b) Time evolution of the q profile.

transition between strong and weak coupling, the poloidal wave number $k_\vartheta = m/r_0$, with r_0 being the radial location of $q_{\rm min}$, satisfies

$$k_\vartheta x_s \approx (k_\vartheta^2/B_{\rm s}' S_{\rm Hp})^{1/9}\,, \tag{3}$$

where $x_{\rm s} = D_{12}/2$, $B_{\rm s}' = s/q_{\rm s}$ and $s = rq'/q$ is the magnetic shear evaluated at a resonant surface. Our conjecture is that, for a fixed x_s, Eq. (3) also gives the transition of the dependence of growth rate on m from an increasing function of m to a decreasing function of m. In other words, directly from Eq. (3), we obtain $m_{\rm peak} = r_0/(x_{\rm s}^9 B_{\rm s}' S_{\rm Hp})^{1/7}$. Based on this conjecture and our extensive numerical analyses, we propose a semi-empirical formula of $m_{\rm peak}$ as

$$m_{\rm peak} \approx r_0/(x_{\rm s}^9 B_{\rm s}' S_{\rm Hp})^{1/7} + 1. \tag{4}$$

Equation (4) is valid for small $x_{\rm s} = D_{12}/2$, where $m_{\rm peak} \gg 1$. For example, for the q profile in Fig. 1(a), where $r_0 = 0.42$, $B_{\rm s}' \approx 0.11$, $x_s \approx 0.03$, one obtains $m_{\rm peak} = 8, 6, 5$ from Eq. (4) for $S_{\rm Hp} = 10^6, 10^7, 10^8$, respectively, which agree with numerically obtained values of $m_{\rm peak}$ under the same conditions. Nonlinear simulations indicate that $m_{\rm peak}$ reliably determines the size of the magnetic island structures when the initial perturbation is random.

3.2. Nonlinear Dynamics

For a random-phase broad-band perturbation, the modes reaching the nonlinear regime first are typically those with $m \sim m_{\rm peak}$. When their amplitudes are sufficiently large, their nonlinear coupling may drive slower eigenmodes. For instance, $(m, n) = (8, 4)$ and $(10, 5)$ couple to produce a $(2, 1)$ component. In general, the driven mode satisfies $m' = m_1 \pm m_2$ (similar for n) and acquires a large growth rate $\gamma_{\rm drive}(m') = \gamma_{\rm lin}(m_1) + \gamma_{\rm lin}(m_2)$. Here, m_1 and m_2 are the driving modes. Such three-mode interactions appear to be the dominant dynamics in the early nonlinear regime for spectra similar to those in Fig. 1(b). For example, a fast growth of the $m = 1$ internal kink mode is shown to be driven by $q_{\rm s} = 1$ TTMs in Section 4.1.

In the fully nonlinear regime, the fast growing high-m modes produce small magnetic islands and an annular collapse occurs in the inter-resonance region. A significant difference between the collisional and collisionless case is observed in the reconnection dynamics: collisionless reconnection permits *multiple* reconnection cycles, as can be observed in Fig. 2(a). Secondary reconnection was demonstrated numerically by Biskamp and Drake [12] for the $m = 1$ internal kink-tearing mode. The results in Fig. 2 show that collisionless DTMs behave in a similar way. In the collisionless case the annular collapse eventually raises q above $q_\mathrm{s} = 2$, leading to a stable relaxed state, as can be seen in Fig. 2(b). In the collisional case, resistive decay of the profile perturbation ($m = 0$ mode) keeps q_min close to or slightly below $q_\mathrm{s} = 2$. Here the systems settles down in a state of balance between continued weak MHD activity and the tendency of the resistive dissipation to drive the system back to its original unstable state.

3.3. Interaction with Sheared Zonal Flows

Motivated by experimental evidence of strongly sheared zonal flows in the vicinity of q_min in ERS discharges [13] and their possible relevance for the formation of an internal transport barrier (ITB) [1], effects of shear flows on resistive MTMs have been investigated. It has been shown in Ref. [14] that, for $q_\mathrm{s} = 2$ DTMs, (a) higher-m DTMs may remain dominant even in the presence of significant shear flow, and (b) sufficiently strong shear flow itself may destabilize high-m modes near q_min. The linear growth rates of shear flow driven modes are independent of resistivity. In the nonlinear regime, small but finite resistivity allows magnetic reconnection to occur. During the further evolution the flows and the magnetic structures become increasingly turbulent. The results also indicate that, with sufficiently small resistivity, the flattening of the q profile takes significantly longer than the flattening of the flow profile, so that the latter becomes the primary nonlinear saturation mechanism.

4. $q_\mathrm{s} = 1$ Triple Tearing Modes (TTMs)

The results obtained for DTMs may be applied to configurations with more than two resonant surfaces. In this section we discuss $q_\mathrm{s} = 1$ triple tearing modes (TTM) [6, 7] for the q profile shown in Fig. 3(a) with three adjacent resonant surfaces r_s1, r_s2 and r_s3. Here we consider the resistive case only ($d_\mathrm{e} = 0$). Of particular interest is the evolution of the $m = 1$ internal kink-tearing mode due to its global mode structure and its relevance to internal disruptions (sawtooth crashes) in tokamak plasmas [15]. The data shown in Figs. 3 and 4 were obtained using 256 modes ($0 \leq m \leq 255$). Although there are some differences in detail, the overall features of the results presented in Ref. [7] (128 modes) are reproduced.

4.1. Fast trigger for the $m = 1$ mode

Let us now examine the nonlinear evolution of the $m = 1$ mode shown in Fig. 3(b). After the linear phase of growth [stage (i) in Fig. 3(b)] the growth rate of the $m = 1$ mode increases significantly to a value that, in the present example, is an order of magnitude larger than the linear growth rate [stage (ii) in Fig. 3(b)]. As mentioned in Section 3.2., this is due to nonlinear driving by fast growing high-m modes. Nonlinear coupling between m_peak and its immediate sidebands drives the $m = 1$ perturbation. Due to this enhanced growth the $m = 1$ mode reaches an observable magnitude much faster than would be

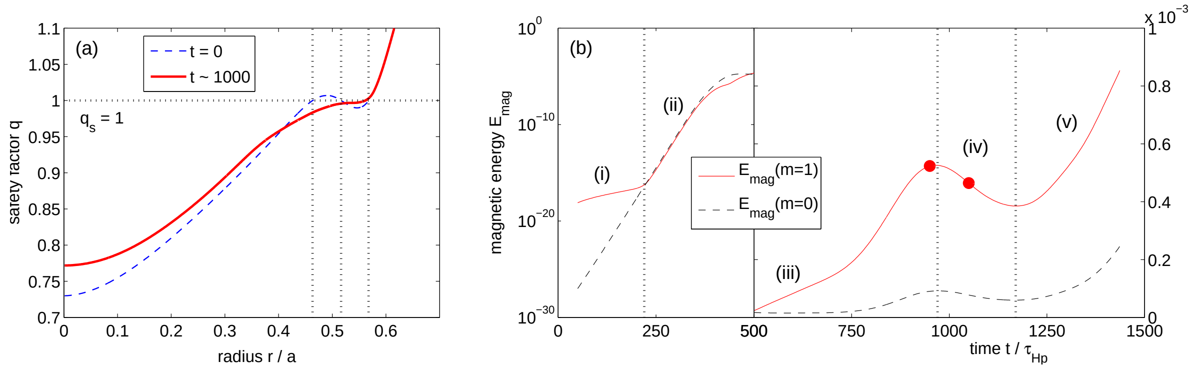

Figure 3: (a): Equilibrium q profile with three $q_s = 1$ resonances and locally flattened profile just after the kink flow reversal. (b): Evolution of the magnetic energy E_{mag} of the $m = 1$ and $m = 0$ modes.

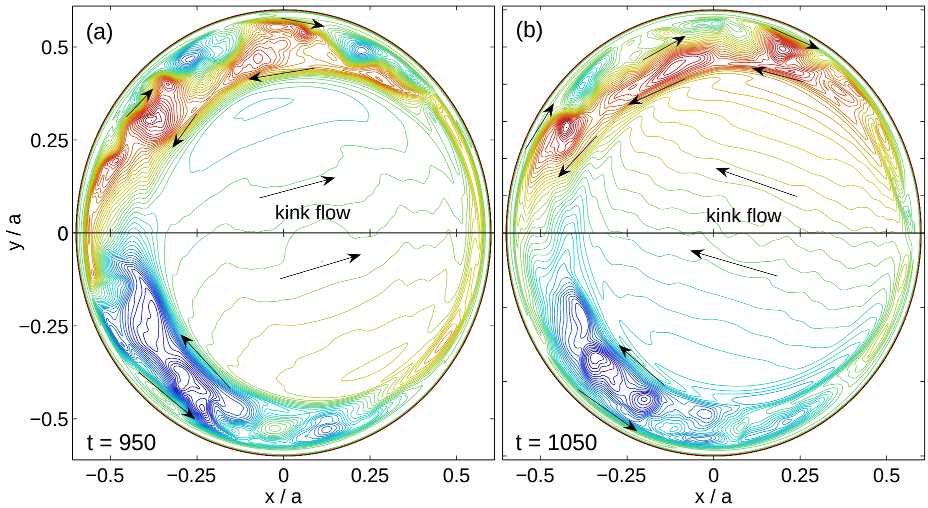

Figure 4: Potential contours showing the $\mathbf{E} \times \mathbf{B}$ flows before and after the nonlinear saturation of the internal kink mode. Arrows indicate the instantaneous flow directions.

expected from its linear growth rate. Although the driving occurs only in a radially localized region $r_{s1} \lesssim r \lesssim r_{s3}$, the *whole* global $m = 1$ mode ($0 \leq r \leq r_{s3}$) grows at an enhanced rate. Therefore, it is proposed that this driving mechanism may explain the fast trigger of the sawtooth crash [6], provided that multiple $q_s = 1$ resonant surfaces are present.

4.2. Saturation of the $m = 1$ mode

Since $q < 1$ in the region $0 < r < r_{s1}$ the entire core plasma can undergo magnetic reconnection. In resistive RMHD simulations with monotonic q profiles (single $q_s = 1$ resonant surface) this *full reconnection* seems to be inevitable [15], at least when pressure effects and diamagnetic drifts are neglected [16]. In the presence of multiple $q_s = 1$ resonances, however, *partial reconnection* may occur [6, 7]. Here, fast growing high-m TTMs induce an annular collapse in the inter-resonance region $r_{s1} \lesssim r \lesssim r_{s3}$ before the global $m = 1$ mode can grow to a significant amplitude. The q profile is annularly flattened and the following dynamics in the disrupted belt around the core is governed by a burst of MHD turbulence. It has been shown that this turbulence is capable of changing the direction of core displacement, impeding the growth of the $m = 1$ mode, and even making it decay [7]. An example for such a scenario is shown in Fig. 3(b): phase (iii) indicates the annular collapse, (iv) the saturation and reversal of the kink flow, and (v) resumption of the sawtooth crash. The snapshots in Fig. 4(a) and (b) were taken just before and after the reversal of the kink flow. The simulation results have indicated that motion of the kink sensitively depends on the initial perturbation and state of turbulence in the disrupted region. As in the example in Fig. 3(b), at later times full reconnection is usually observed (similar to a compound sawtooth crash [17]). The relevant point to be made here is that there is a significant interaction between the global $m = 1$ mode and the surrounding turbulent belt.

5. Discussion

In this paper, we have presented our recent results on current-driven MHD instabilities near $q_{\rm min}$ in reversed-shear configurations. More specifically, based on an RMHD model with electron inertia, collisional and collisionless high-m DTMs were studied. A better understanding of DTMs may facilitate a better control of ERS tokamak discharges, where an ITB is created near $q_{\rm min}$ and may provide the plasma with an access to the regime of improved confinement [18]. DTMs may also play a significant role for disruptions or disruption control [19]. Nonlinear interaction of the $m = 1$ internal kink mode with MHD turbulence generated by high-m TTMs has also been examined. The simulation results presented here provide possible mechanisms of certain features of sawtooth crashes, such as sudden onset of the internal disruption and partial sawtooth crashes (e.g., Ref. [4]).

The simplicity of the RMHD model used in this study has allowed us to understand fundamental properties of tokamak plasmas in the presence of high-m MTMs in a relatively simple manner. Inclusion of more realistic effects, such as neoclassical effects [20, 21] and kinetic effects, is an important next step toward more quantitative prediction of nonlinear dynamics of MTMs in tokamak plasmas.

Acknowledgments

A.B. would like to thank Y. Kishimoto, Y. Nakamura, and F. Sano at Kyoto University, and S. Günter and E. Strumberger at the Max-Planck-Institut für Plasmaphysik (IPP) in Garching for valuable discussions. He also acknowledges the IPP Garching for its support and hospitality. S.B. acknowledges the Graduate School of Energy Science at Kyoto University and the Center for Atomic and Molecular Technologies at Osaka University for their support and hospitality under visiting professorships. S.H. acknowledges the University of Provence for support and hospitality under visiting professorship. This work was partially supported by the 21st Century COE Program at Kyoto University and Japan-France Integrated Action Program "SAKURA" for Osaka University and the University of Provence.

References

[1] J. W. Connor *et al.* A review of internal transport barrier physics for steady-state operation of tokamaks. *Nuclear Fusion*, 44:R1, 2004.

[2] H. P. Furth *et al.* Tearing mode in the cylindrical tokamak. *Phys. Fluids*, 16(7):1054, 1973.

[3] B. Coppi *et al.* Resistive internal kink modes. *Fiz. Plazmy*, 2:961, 1976. [Sov. J. Plasma Phys. **2**, 533 (1976)].

[4] F. Porcelli *et al.* Predicting the behavior of magnetic reconnection processes in fusion burning plasma experiments. *Nucl. Fusion*, 44:362, 2004.

[5] A. Bierwage *et al.* Fast growing double tearing modes in a tokamak plasma. *Phys. Plasmas*, 12(8):082504, 2005.

[6] A. Bierwage *et al.* Nonlinear evolution of $q = 1$ triple tearing modes in a tokamak plasma. *Phys. Rev. Lett.*, 94(6):065001, 2005.

[7] A. Bierwage *et al.* Nonlinear evolution of $m = 1$ internal kinke modes in the presence of magnetohydrodynamic turbulence. *Phys. Plasmas*, 13(3):032506, 2006.

[8] H. R. Strauss. Nonlinear, three-dimensional magnetohydrodynamics of noncircular tokamaks. *Phys. Fluids*, 19(1):134, 1976.

[9] A. Bierwage *et al.* Dynamics of resistive double tearing modes with broad linear spectra. Preprint: http://arxiv.org/abs/physics/0609115.

[10] A. Bierwage and Q. Yu. Comparison between resistive and collisonless double tearing modes for nearby resonant surfaces.
Preprint: http://arxiv.org/abs/physics/0609102.

[11] P. L. Pritchett *et al.* Linear analysis of the double-tearing mode. *Phys. Fluids*, 23(7):1368, 1980.

[12] D. Biskamp and J. F. Drake. Dynamics of the sawtooth collapse in tokamak plasmas. *Phys. Rev. Lett.*, 73(7):971, 1994.

[13] R. E. Bell *et al.* Poloidal rotation in TFTR reversed shear plasmas. *Phys. Rev. Lett.*, 81(7):1429, 1998.

[14] A. Bierwage *et al.* Large-mode-number mhd instability driven by sheared flows in reversed-shear tokamak plasmas.
Submitted. Preprint: http://arxiv.org/abs/physics/0607196.

[15] B. B. Kadomtsev. Disruptive instability in tokamaks. *Sov. J. Plasma Phys.*, 1:153, 1975.

[16] Y. Nishimura *et al.* Onset of high-n ballooning modes during tokamak sawtooth crashes. *Phys. Plasmas*, 6(12):4685, 1999.

[17] H. R. Koslowski *et al.* Characteristics of the q profile for different confinement conditions in TEXTOR-94. *Plasma Phys. Controlled Fusion*, 39:B325, 1997.

[18] S. Günter *et al.* MHD phenomena in reversed shear discharges on ASDEX Upgrade. *Nucl. Fusion*, 40(8):1541, 2000.

[19] Y. Ishii *et al.* Long timescale plasma dynamics and explosive growth driven by the double tearing mode in reversed shear plasmas. *Nucl. Fusion*, 43:539, 2003.

[20] Q. Yu. Nonlinear evolution of neoclassical double tearing mode. *Phys. Plasmas*, 4(4):1047, 1997.

[21] Q. Yu and S. Günter. Numerical modelling of neoclassical double tearing modes. *Nucl. Fusion*, 39(4):487, 1999.